ELSEVIER

Journal of Chromatography A, 876 (2000) 51–62

JOURNAL OF CHROMATOGRAPHY A

www.elsevier.com/locate/chroma

Optimization of ion-exchange displacement separations I. Validation of an iterative scheme and its use as a methods development tool

Venkatesh Natarajan, B. Wayne Bequette, Steven M. Cramer*

Department of Chemical Engineering, Rensselaer Polytechnic Institute, Troy, NY 12180, USA

Received 26 July 1999; received in revised form 7 January 2000; accepted 26 January 2000

Abstract

Displacement chromatography has been demonstrated to be a powerful, high-resolution preparative tool. The performance of displacement systems can be affected by a variety of factors such as the feed load, flow-rate, initial salt concentration and the displacer partition ratio. Thus, the optimization of displacement separations is a uniquely challenging problem. In this manuscript, an iterative optimization scheme has been presented whereby one can identify the optimum operating conditions for displacement separations at a given level of loading on a given resin material. The solid film linear driving force model has been employed in concert with the Steric Mass Action formalism of ion-exchange chromatography to describe the chromatographic behavior in these systems. Simple pulse techniques have been employed to estimate the transport parameters. The iterative scheme has been validated using a rigorous Feasible Sequential Quadratic Programming algorithm. Finally, the utility of the iterative optimization scheme as a methods development tool for displacement separations has been demonstrated for a difficult separation. The results indicate that the use of the optimization scheme leads to significantly better performance than standard rules of thumb.

Keywords: Optimization; Displacement chromatography; Steric mass action; Ion-exchange chromatography

1. Introduction

Ion exchange chromatography is widely employed as a preparative purification tool in the biotechnology industry. While gradient elution is most commonly employed to separate proteins, it is often necessary to reduce column loadings to maintain the resolving power of gradient chromatography. Displacement chromatography, on the other hand, has been demonstrated to be efficacious even with extremely difficult separation problems [1].

The optimization of displacement separations of macromolecules poses a difficult problem. The yields obtainable in displacement systems are a strong function of the thickness of the shock layers, which in turn, depend on the particle size, flow-rate and the degree of difficulty of the separation [2]. To accurately account for these effects one needs to have appropriate mass transport and adsorption models.

Traditionally, the Langmuir isotherm has been employed to describe adsorption in ion-exchange systems. Unfortunately, this approach cannot describe the effect of the salt concentration on the adsorption behavior of the solutes in multicomponent ion-exchange chromatography. Furthermore, it does

*Corresponding author. Tel.: +1-518-276-6198; fax: +1-518-276-4030.

0021-9673/00/$ – see front matter
PII: S0021-9673(00)00138-2

not account for the multipointed nature of protein adsorption. A multivalent ion-exchange formalism has been proposed and employed successfully to describe the salt dependence of adsorption in ion-exchange systems [3,4]. It combines the stoichiometric displacement model [5,6] with the electroneutrality condition to describe the ion-exchange of solutes. However, in the case of macromolecules such as proteins, steric effects and lateral interactions are expected to play an important role [7–10]. The Steric Mass Action (SMA) model of ion-exchange chromatography incorporates the effects of salt and steric shielding on protein binding in ion-exchange systems [9]. Raje and Pinto [11] have recently shown that the steric factor in the SMA model can include both the effects of steric shielding and lateral interactions. This model has been shown to accurately predict single component and multicomponent ion-exchange chromatographic behavior in isocratic [12], gradient [13,14] and displacement chromatography [15].

For a complete description of the chromatographic behavior of a solute, one needs to use an appropriate transport model in conjunction with the adsorption isotherm. The solid film linear driving force model has been employed to describe the shock layers in non-linear chromatographic systems [2,16]. Recently, it has been demonstrated that the solid film linear driving force model can be used in conjunction with the SMA formalism to accurately describe shock layers in protein ion-exchange displacement systems over a wide range of operating conditions [17].

Several researchers have addressed the problem of optimizing displacement separations. Frenz et al. [18] carried out an experimental study of the dependence of the throughput on operational parameters in reversed-phase displacement systems. Jen and Pinto [19] employed the Coherence theory of multicomponent chromatography to optimize ideal displacement separations. Felinger and Guiochon [20] employed a modified simplex algorithm to carry out the optimization of experimental conditions in displacement systems. However, they employed the equilibrium-dispersive model that restricts their results to stationary phase materials with relatively small particle sizes (5–20 μm).

In this manuscript, the solid film linear driving force model will be employed in concert with the SMA isotherm and appropriate boundary conditions to describe displacement separations. A novel iterative algorithm to optimize displacement separations on various stationary phase materials is presented. This algorithm is validated and its use as a methods development tool is demonstrated.

2. Theory

2.1. Chromatographic optimization

To accomplish the optimization of non-linear, preparative chromatographic systems, one needs to keep in mind four different factors: objective function, parameters, decision variables and constraints [13]. A brief description of each factor is presented below.

2.1.1. Objective function

Optimization consists of maximizing or minimizing a given objective function. While there are several possible objective functions (e.g. cost, yield, etc.), the most commonly employed objective function in preparative chromatography is the production rate which is defined as follows:

$$PR_i = \frac{C_{i,\mathrm{f}} V_{\mathrm{f}} Y_i}{t_{\mathrm{cyc}} V_{\mathrm{sp}}} \tag{1}$$

where PR is the production rate of the ith component, $C_{i,\mathrm{f}}$ is the feed concentration, V_{f} is the feed volume, Y_i is the yield, t_{cyc} is the cycle time and V_{sp} is the stationary phase volume. The production rate is a measure of the amount of protein purified per unit time and per unit stationary phase volume. In order to compute the production rate, the yield needs to be calculated. In displacement systems, unlike gradient systems, there is never a baseline separation (unless selective displacement is carried out [21]). The following equation was employed to calculate the yield:

$$Y_i = \frac{\int_{t_1}^{t_2} C_i \, \mathrm{d}t}{C_{i,\mathrm{f}} t_{\mathrm{f}}} \tag{2}$$

where the cut-times t_1 and t_2 are chosen to maximize the yield for a given level of purity.

2.1.2. Parameters

Parameters cannot be changed during the optimization process. The typical parameters in a preparative chromatographic system are the feed constituents and their relative compositions, the stationary phase material and the pH at which the separation is carried out.

2.1.3. Decision variables

These are the variables that are actually changed during the optimization process. The typical decision variables are the feed load, the salt concentration, flow-rate and Δ. In all optimizations in this manuscript, the salt concentration, flow-rate and Δ were treated as the decision variables.

In this study, it was assumed that the separation was carried out at the pH at which maximum selectivity was obtained on a given resin system. Thus, the pH of the separation was treated as a parameter and not as a decision variable.

2.1.4. Constraints

Constraints define the regions of the operating space in which the optimization process can be carried out. They may be physical constraints such as solubility constraints or quality constraints such as yield and purity. The constraints employed in this study are: purity, yield and maximum protein concentration. The maximum purity constraint needs to be imposed so that one does not end up with conditions which result in the precipitation of the feed components during the separation process. On the other hand, purity and the yield constraints are dictated by the desired quality of the product and the efficiency of the displacement separation. In all optimizations in this manuscript, a solubility constraint in the form of a maximum protein concentration of 4 m*M* was imposed. In addition, purity constraints ($>$95% purity) and yield constraints ($>$80% yield) were also imposed.

2.2. Steric Mass Action formalism

The SMA formalism is a three-parameter model [9] for the description of multicomponent protein–salt equilibrium in ion-exchange systems. The multipointed binding of the protein molecule to the stationary phase is represented as a stoichiometric exchange of mobile phase protein and bound counter ions as follows:

$$C_i + \nu_i \bar{Q}_1 \Leftrightarrow Q_i + \nu_i C_1 \tag{3}$$

where ν_i is the characteristic charge of the protein, the subscript 1 represents the salt counter ion, C_i and Q_i are the mobile phase and stationary phase concentrations of component i and $\bar{Q}_1$ is the number of sites on the stationary phase available for exchange with the protein. The equilibrium constant for the above reaction is given by:

$$K_i = \left(\frac{Q_i}{C_i}\right)\left(\frac{C_1}{\bar{Q}_1}\right)^{\nu_i} \tag{4}$$

In addition to binding to ν_i sites, each adsorbed protein molecule will also sterically shield σ_i counter ions on the stationary phase. The number of counter ions blocked by a particular protein will be proportional to the concentration of the protein on the adsorptive surface [8].

$$\hat{Q}_i = \sigma_i Q_i \tag{5}$$

The steric factor, σ, describes the non-linear adsorption behavior of the proteins. On the other hand, the equilibrium constant K and the characteristic charge ν describe the linear adsorption behavior of the proteins.

An ion-exchange surface must maintain electroneutrality. This is given by the following equation for a multicomponent mixture:

$$\Lambda = \bar{Q}_1 + \sum_{i=2}^{NC} (\nu_i + \sigma_i) Q_i \tag{6}$$

Eqs. (4)–(6) constitute the SMA formalism.

2.3. Mass transport equations

The following solid film linear driving force model was employed to describe the effects of mass transfer limitations in ion-exchange chromatographic systems:

$$\frac{\partial C_i}{\partial \tau} + \beta \frac{\partial Q_i}{\partial \tau} + \frac{\partial C_i}{\partial x} = \frac{1}{Pe_i} \frac{\partial^2 C_i}{\partial x^2} \tag{7}$$

$$\frac{\partial Q_i}{\partial \tau} = St_i(Q_i^* - Q_i) \qquad i = 1, \ldots, NC \tag{8}$$

where Pe_i is the Peclet number and St_i is the Stanton number of the ith component and Q_i^* is the equilibrium stationary phase concentration of the ith component. The Peclet number describes the effect of axial dispersion on the system and the Stanton number is a lumped parameter describing both the external film mass transfer resistance and the pore diffusion limitations.

2.4. Numerical solution of model equations

Finite difference techniques were employed to solve Eqs. (7) and (8). As the SMA isotherm is implicit, a Newton–Raphson technique was used in each step for the equilibrium calculations. The temporal terms were discretized using forward differences while the convection and diffusion terms were discretized using backward and central differences, respectively.

The discretized equations were solved subject to the following stability criteria [17]:

$$\frac{\Delta\tau}{Pe_i(\Delta x)^2} < 0.2 \tag{9}$$

$$\frac{\Delta\tau}{\Delta x} < 1 \tag{10}$$

A FORTRAN code was written to solve the above mentioned equations. The program was run on an IBM RS/6000 workstation using IBM FORTRAN under the AIX 4.0 operating system.

2.5. Optimization technique

Optimization of displacement separations involves four decision variables: feed load, initial salt concentration, flow-rate and Δ. The Feasible Sequential Quadratic Programming algorithm (FSQP) of Zhou and Tits [22] is a set of subroutines for the minimization of a smooth objective function subject to nonlinear smooth inequality constraints, linear inequality and equality constraints, and simple bounds on the variables. FSQP uses a Sequential Quadratic Programming (SQP) algorithm. Given a feasible iterate x, the basic SQP direction, d^0, is first computed by solving a standard quadratic problem using a positive definite estimate H of the Hessian of the Lagrangian. Next, an essentially arbitrary feasible direction $d^1 = d^1(x)$ is computed and for a certain scalar ρ, a feasible descent direction $d = (1-\rho)d^0 + \rho d^1$ is obtained. Finally, a correction d^2 is computed and a search is performed along the arc $x + td + t^2d^2$. FSQP can be employed to either solve a full optimization problem or generate feasible points. In this manuscript, it was employed to carry out the simultaneous optimization of the flow-rate and Δ at a given level of loading in displacement systems.

In addition, a novel iterative algorithm was developed to accomplish the rapid optimization of displacement separations. Fig. 1 illustrates the algorithm which is discussed in detail later in the manuscript.

3. Experimental

3.1. Materials

Sodium monobasic phosphate, sodium dibasic phosphate, horse cytochrome C, bovine cytochrome C and neomycin sulfate were purchased from Sigma Chemical (St. Louis, MO). Sodium chloride was purchased from Aldrich Chemical (Milwaukee, WI). *o*-Phosphoric acid was purchased from Fisher Scientific (Rochester, NY). The strong cation-exchange column was packed with Waters SP stationary phase material (polymethyl methacrylate backbone, nominal pore diameter of 1000 Å, sulfopropyl, 40 μm) The strong cation-exchange column used for protein analysis (polymethyl methacrylate backbone, nominal pore diameter of 1000 Å, sulfopropyl, 8 μm, 0.5×5 cm) was obtained from Waters Corporation (Milford, MA).

3.2. Apparatus

All displacement experiments were carried out using a Model 590 programmable HPLC pump (Waters, Milford, MA) connected to the chromatographic columns via a Model C10W 10-port valve (Valco, Houston, TX, USA). Data acquisition and processing were carried out using a Millenium 2010

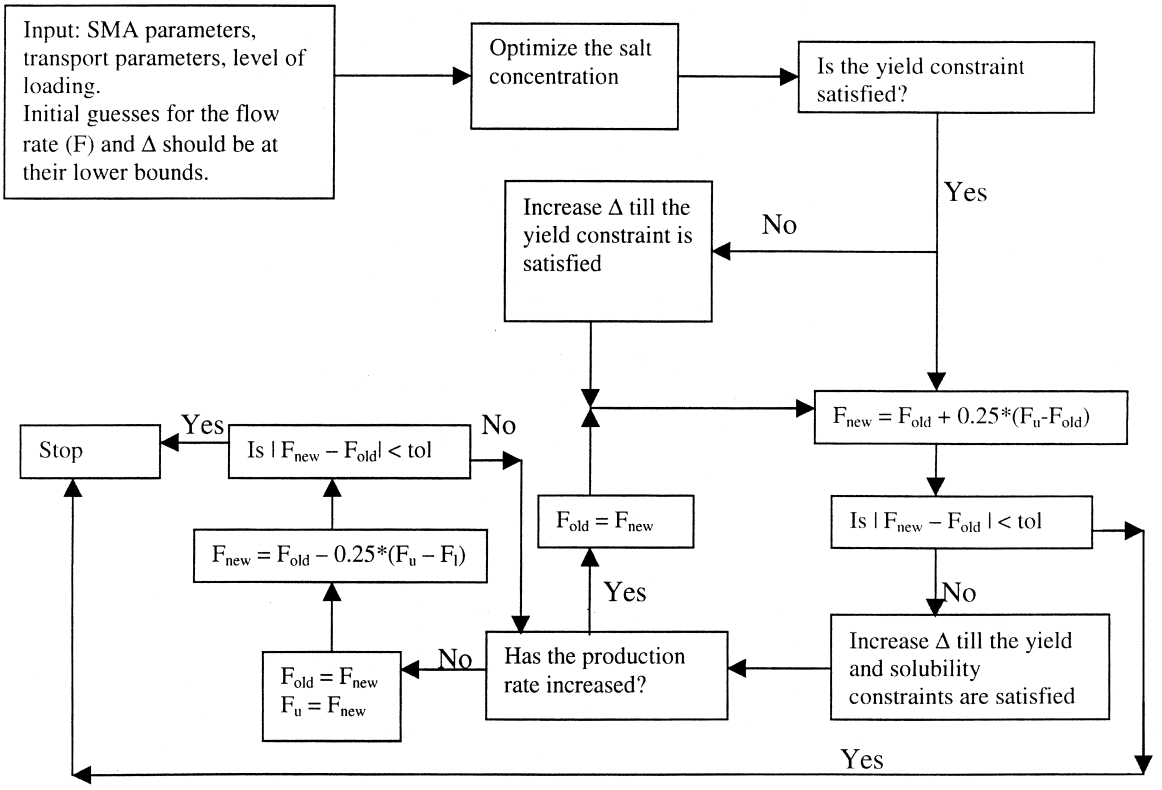

Fig. 1. Iterative scheme for optimizing displacement separations.

chromatography workstation (Waters). Fractions of the column effluent were collected using LKB 2212 Helirac fraction collector (LKB, Sweden). Protein analysis for the collected fractions were carried out using a WISP model 712 autoinjector (Waters) connected to a model 650E Advanced Protein Purification system (Waters) with a model 484 Tunable Absorbance Detector (Waters). UV absorbance of samples was measured on a Lambda 6 UV–Vis spectrophotometer (Perkin-Elmer).

3.3. Procedures

3.3.1. Estimation of SMA parameters of proteins

The linear SMA parameters of the proteins (K and ν) were determined using the protocols outlined by Gadam et al. [23]. Briefly, the characteristic charge and the equilibrium constant were determined using linear elution retention data at different mobile phase salt concentrations. The non-linear parameter (σ, steric factor) was obtained from frontal experiments carried out at a single salt concentration (typically, <100 mM) and at a low flow-rate.

3.3.2. Estimation of SMA parameters of displacers

The characteristic charge of the displacer was determined from the induced salt gradient produced from passing a front of the displacer at a known concentration. The equilibrium constant and the steric factor was then determined by a best fit of the adsorption isotherms of the displacer obtained at various mobile phase salt concentrations [24].

3.3.3. Estimation of the mass transport properties of proteins

Pulse techniques under retained and unretained conditions were employed to characterize the mass transport properties of the proteins on the various stationary phases. The interstitial porosity was determined independently using a pulse of blue dextran

and the particle porosity was computed from the elution times of the unretained protein pulses. The second moment of the elution profiles were employed to estimate the column plate height (HETP). For further details, the reader is referred to Natarajan and Cramer [25].

3.3.4. Estimation of the mass transport properties of the displacer

The mass transfer parameters of the displacers were obtained by a least squares fit of the breakthrough curves of the displacers at two different flow-rates [17].

3.3.5. Displacement experiments

The column was initially equilibrated with the carrier and then subsequently perfused with feed, displacer and regenerant solutions. The feed load, salt concentration and displacer concentration employed for the separation are given in the figure legends of the respective chromatograms. Fractions of 200 μl were collected for subsequent analysis of protein and displacer concentration in the effluent.

3.3.6. Protein analysis

Analysis of the fractions collected during the displacement experiments was performed by cation-exchange HPLC under isocratic conditions. The fractions were diluted 5–100 fold. A mobile phase of 50 m*M* sodium phosphate, pH 6, containing 75 m*M* sodium chloride was employed for the analysis of bovine and horse cytochrome C. The proteins were detected using a UV–Vis detector at 280 nm.

3.3.7. Displacer analysis

Neomycin sulfate was analyzed using a phenol–sulfuric acid assay [26]. The fractions were diluted 5–20 fold. A sample volume of 0.8 ml was mixed with 3.2 ml of sulfuric acid, reacted for 1 min, and cooled to room temperature. A 50 μl volume of 90% phenol (w/v) was then added and the resultant mixture allowed to equilibrate for 30 min. The absorbance was read at 480 nm.

4. Results and discussion

4.1. The effect of salt concentration

A series of simulations was initially carried out on a binary feed mixture whose parameters are presented in Table 1. Fig. 2a and b present the yield of the more retained solute (solute 2) as a function of salt concentration at a fixed flow-rate. These parametric plots were generated at low (Fig. 2a) and high (Fig. 2b) loadings at various Δ's (where $\Delta = Q_{disp}/C_{disp}$, the displacer partition ratio). As can be seen in Fig. 2, the qualitative shape of these curves is dependent solely on the feed loading and is independent of the Δ. In order to understand this behavior, representative simulated chromatograms are shown in Fig. 3. Fig. 3a–c illustrates the effect of the initial salt concentration on the yields in a displacement process. At low salt concentrations, the concentrations of the displaced proteins are high and the solute zones are narrow (Fig. 3a). Thus, the fraction of the solute zone occupied by the shock layer region is higher, resulting in a concomitant reduction in yield. Upon increasing the salt concentration (Fig. 3b), the concentrations of the displaced proteins decreases, resulting in broader solute zones and concomitantly higher yields. Upon further increasing the salt concentration, non-development occurs and the yield again starts decreasing (Fig. 3c). The results shown in Figs. 2 and 3 suggest that the location of the optimum salt concentration for displacement chromatography is dependent only on the level of loading. At different Δ's, the location of the optimum salt concentration does not change; only the yields change (Fig. 2). Since the effect of the salt concentration is more pronounced at lower Δ (which corresponds to higher displacer concentration), one only needs to fix the Δ at a low value in order to

Table 1
Parameters used for simulations presented in Figs. 2 and 3 ($\Lambda = 590$ m*M*, $\epsilon_t = 0.70$)

Solute	ν	K	σ	k_m (min^{-1})
Solute 1	5	0.006	40	100
Solute 2	5.2	0.006	40	100
Displacer	4.0	10	3.5	200

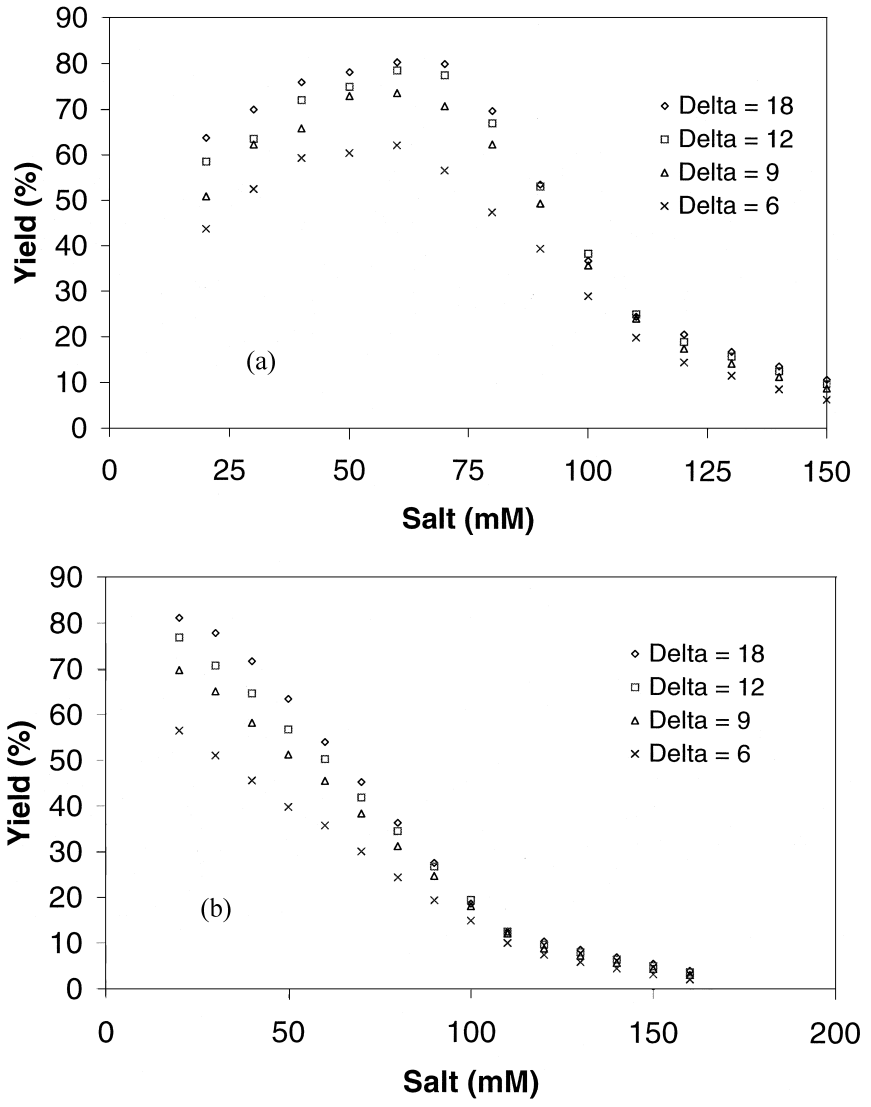

Fig. 2. Dependence of the optimum initial salt concentration on the feed load and Δ. The plots were generated using the parameters listed in Table 1. (a) Feed load = 0.50 column volumes. (b) Feed load = 1 column volume.

identify the optimum salt concentration at a given level of loading.

These results enable the construction of a rapid iterative scheme for the optimization of displacement separations at a given level of loading. Such a scheme is outlined in Fig. 1. As can be seen in the figure, the overall optimization problem has been divided into two simpler optimization problems: (a) the optimization of the salt concentration and (b) optimization of the flow-rate and Δ.

The optimization scheme begins with the flow-rate and Δ set at their respective lower bounds (note: the lower bound for Δ is based on a breakthrough of two column volumes). Following this, the initial salt concentration is optimized using the bisection method. Having optimized the salt concentration, the

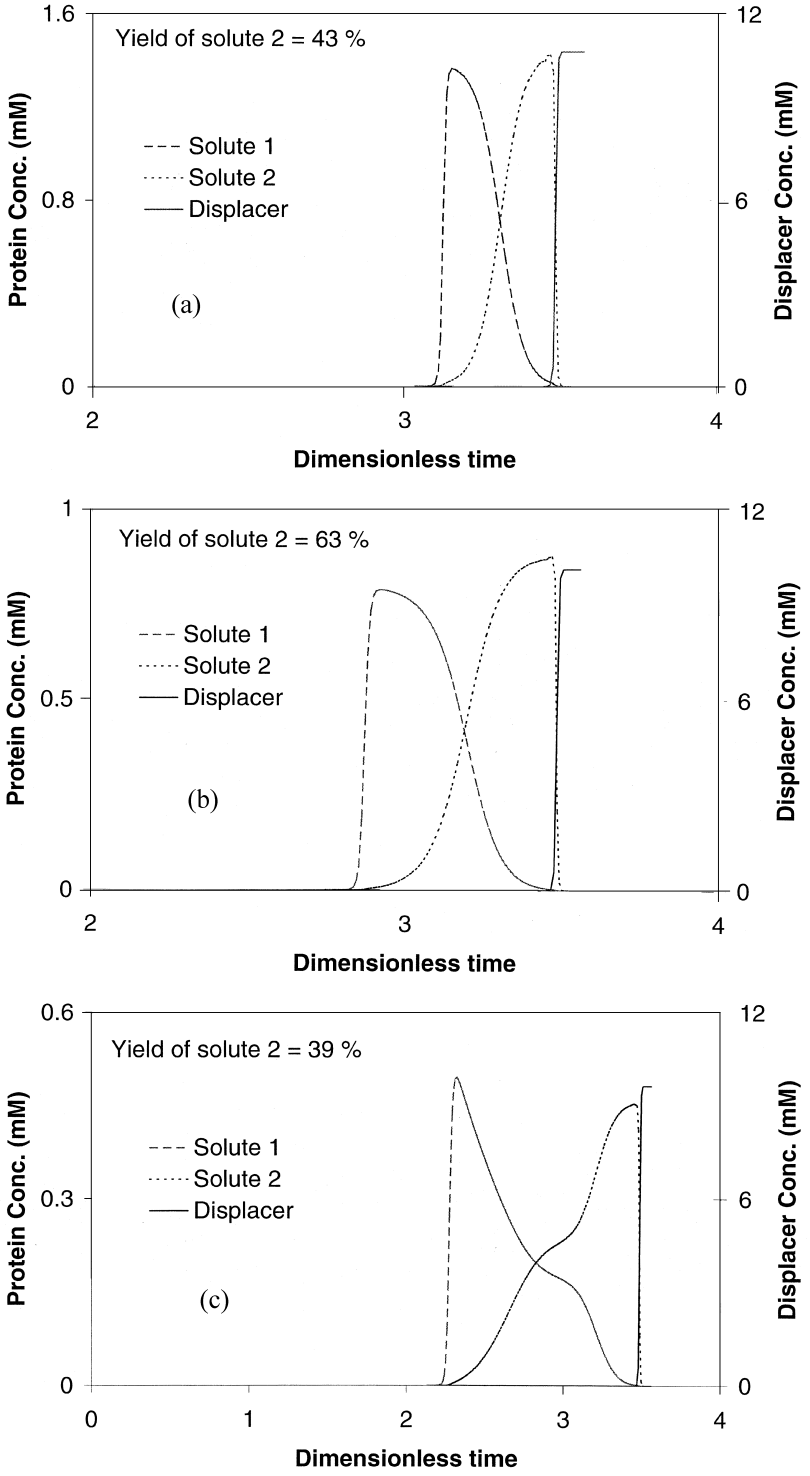

Fig. 3. Simulated chromatograms illustrating the influence of the initial salt concentration on the yield of solute 2. The simulations were carried out with the parameters listed in Table 1. The feed load in all the three cases = 0.5 column volumes and the Δ in all the three cases = 7. (a) Initial salt = 20 m*M*, (b) 50 m*M*, (c) 110 m*M*.

Table 2
Parameters of test problem used for comparison of iterative and FSQP algorithms ($\Lambda = 590$ mM, $\epsilon_t = 0.70$)

Solute	ν	K	σ	k_m (min^{-1})
Solute 1	5.5	0.006	40	100
Solute 2	6.0	0.007	40	100
Displacer	4.0	10	3.5	200

scheme then proceeds to simultaneously optimize the flow-rate and Δ. As seen in Fig. 1, the flow-rate and Δ are systematically varied to maximize the production rate given the constraints of yield (calculated at >95% purity) and solubility. An important concept employed in this scheme is that the solubility and yield constraints can be satisfied by increasing Δ (i.e. decreasing the displacer concentration) and that the yield constraint can also be satisfied by decreasing the flow-rate. While the scheme shown in Fig. 1 is for a fixed level of loading, it can also be repeated at various loadings to determine the optimum feed load for a given displacement separation.

4.2. Validation of the iterative portion of the optimization scheme

The iterative scheme for the simultaneous optimization of the flow-rate and Δ was validated using a test problem (see Table 2) and the FSQP routine described above. Constraints of >80% yield at >95% purity were imposed on the system. In addition, a solubility constraint of <4 mM was imposed. The feed composition was fixed at 0.5 mM of each protein. Fig. 4 compares the results using the FSQP algorithm and the iterative optimization algorithm outlined in Fig. 1. As seen in the figure, the results using these two algorithms are in excellent agreement. The advantage of the iterative optimization scheme lies in the substantial reduction in computational time. In the FSQP algorithm, both the Jacobian and the gradient of the objective functions need to be computed using finite differences. This requires at least 12 function calls to make a decision. Each function call involves the solution of a set of PDEs. Hence, the FSQP algorithm can be computationally expensive. On the other hand, the iterative scheme employs a knowledge of the basic physics of the problem and hence results in a significantly lower number of function calls. For challenging separation problems, the time taken by FSQP could be as long as 8–12 h (depending on the level of loading) whereas the iterative scheme could accomplish the same optimization of these difficult separations in 2–4 h.

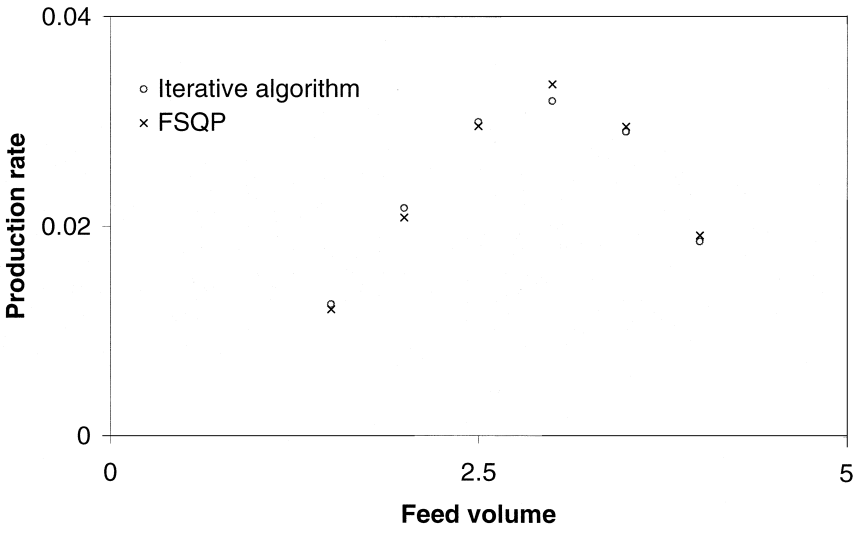

Fig. 4. Comparison of FSQP results and the results obtained using the iterative algorithm outlined in Fig. 1. The initial salt concentration was fixed at 50 mM.

4.3. The optimization scheme as a methods development tool

The utility of the optimization scheme as a methods development tool will now be demonstrated. The separation problem considered here is a mixture of bovine and horse cytochrome C's. The linear retention plots of this mixture are shown in Fig. 5. As is evident from the figure, the mixture poses a very difficult separation problem. Kundu and Cramer [1] have demonstrated that the displacement separation of this mixture yields excellent results on a small particle diameter system. Fig. 6a illustrates the separation of this mixture on a 40 μm Waters resin under conditions normally employed in displacement (i.e. low salt, high displacer concentration (i.e. low Δ) and low flow-rate). As is evident from the figure, the separation is poor and the yield is low. The displaced protein zones are not wide enough to result in pure product. Simulations carried out using parameters shown in Table 3 resulted in good agreement with these experimental results. The iterative optimization scheme (Fig. 1) was employed to determine the optimum conditions for this separation. Fig. 6b compares simulation and experimental results at the optimum conditions. Once again, the comparison between theory and experiment is quite good. In addition, the use of the optimization scheme has resulted in the identification of conditions that can dramatically improve the performance of this process. As can be seen in the figure, the optimum conditions occurred at a lower Δ and a higher salt concentration. These conditions, in turn, led to reduced protein concentrations, and, thus, increased yields. In fact, the lower Δ and higher salt concentrations enabled operation at a higher flow-rate with a concomitant increase in the production rate. It should be pointed out that these conditions are contrary to the several rules of thumb typically employed for displacement separations (e.g. low salt, high displacer concentration and low flow-rates). These results demonstrate the utility of the optimization scheme as a methods development tool for displacement chromatography.

5. Conclusions

In this manuscript, a novel iterative optimization scheme has been presented to carry out the optimization of displacement systems. The optimization routine was validated using a test problem and then applied to a difficult separation problem. The results presented in this paper demonstrate that the optimization scheme can be effectively employed as a methods development tool. In Part II, the optimization scheme will be employed to optimize displacement separations on different resins and, to compare the efficacy of these stationary phase materials for displacement chromatography.

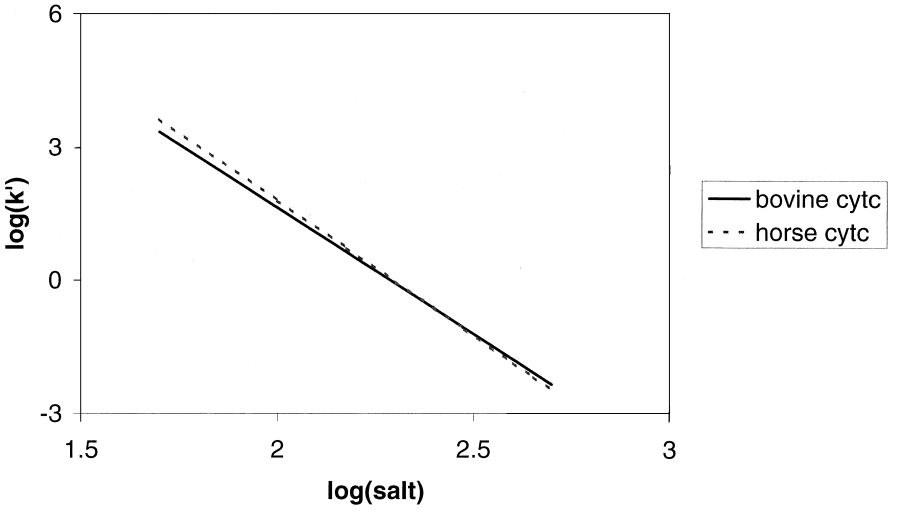

Fig. 5. Linear retention plots for the horse and bovine cytochrome C mixtures on the 40 μm Waters resin.

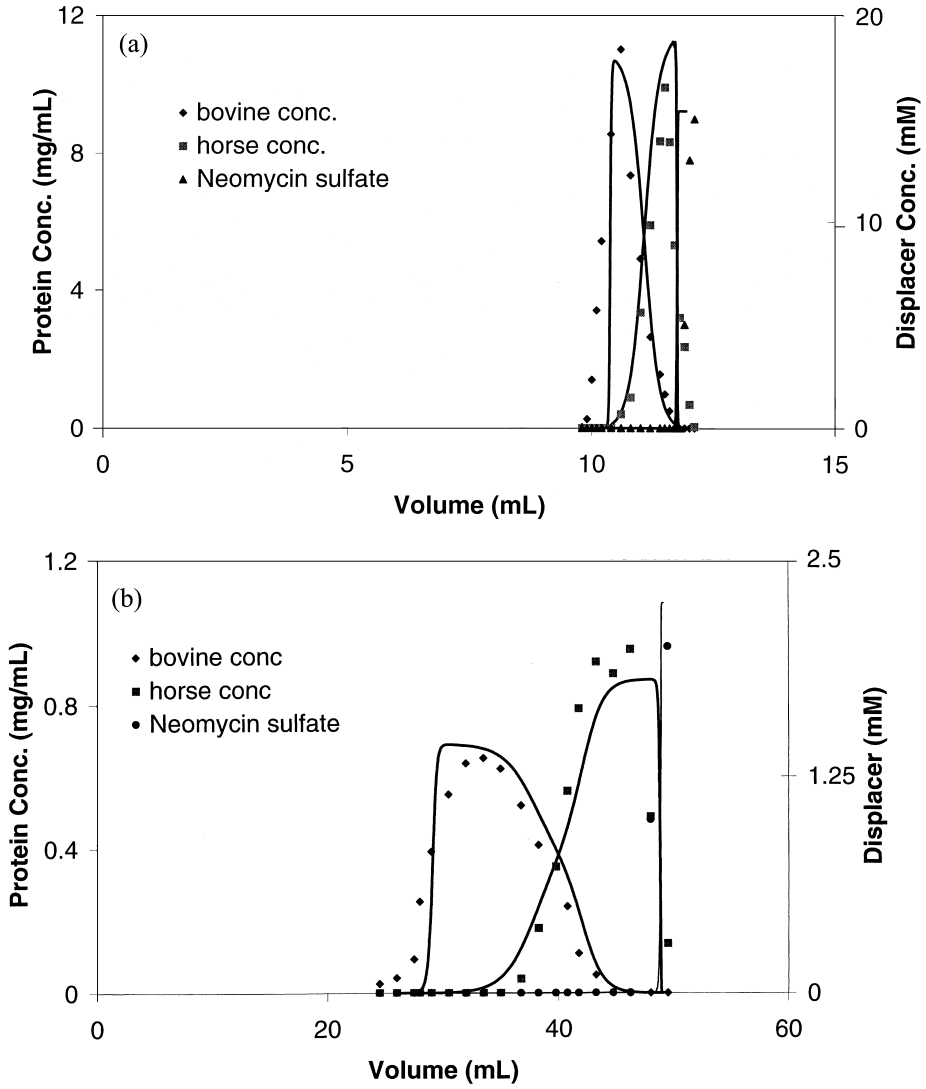

Fig. 6. Displacement separation of the mixture of cyt C's on the 40 μm Waters resin (1 cm I.D.×8 cm). The solid lines are simulation results. (a) Feed load=1.2 ml, feed composition=0.56 m*M* of each protein, flow-rate=0.2 ml/min, initial salt concentration=50 m*M* Na^+ (pH 6), displacer=15 m*M* neomycin sulfate. (b) Feed load=1.2 ml, feed composition=0.56 m*M* of each protein, flow-rate=0.5 ml/min, initial salt concentration=100 m*M* Na^+ (pH 6), displacer=2 m*M* neomycin sulfate.

Table 3
Experimental parameters for simulations of the displacement separation of the cytochrome C's (Λ=525 m*M*, ϵ_t=0.70)

Solute	ν	K	σ	k_m (min^{-1})
Bovine Cyt C	5.9	0.008	45	36
Horse Cyt C	6.3	0.0065	48	36
Displacer	4.0	18.0	3.5	80

6. Nomenclature

C	Mobile phase concentration (m*M*)
C_f	Feed concentration (m*M*)
D	Axial dispersion coefficient (cm^2 min^{-1})
K	Equilibrium constant
k_m	Lumped mass transfer coefficient
L	Length of column (cm)

NC	Number of components in the system
Pe	Peclet number ($=Lu/D$) (dimensionless)
PR	Production rate (mmoles/(ml min))
Q	Stationary phase concentration (=mmoles adsorbed/ml solid-phase) (mM)
Q^*	Stationary phase concentration at equilibrium with C (mM)
$\bar{Q}_1$	Concentration of bound salt that is not sterically shielded (mM)
$\hat{Q}_1$	Concentration of bound salt that is sterically shielded (mM)
St	Stanton number ($=k_m L/u$) (dimensionless)
t	Time (min)
t_o	Time taken for an inert tracer to traverse the column (min)
t_f	Loading time
u	Chromatographic velocity (cm min^{-1}) ($=u_o\varepsilon$)
u_o	Superficial velocity (cm min^{-1})
V_o	Column void volume (ml)
Y	Yield
x	Axial distance along column (dimensionless)

Greeks

β	Phase ratio ($=1-\epsilon/\epsilon$)
ϵ_t	Total porosity
λ	Dynamic affinity
ν	Characteristic charge
σ	Steric factor
τ	Dimensionless time ($=t/t_o$)
τ_f	Dimensionless feed time
Δ	Partition ratio
Λ	Bed capacity (mM)

Subscripts

i	Component number. $i=1$ refers to the salt counterion and $i=NC$ refers to the displacer

Acknowledgements

The authors are grateful to the National Science Foundation (Grant No. CTS-9416921) for funding this research. In addition, the authors would like to thank Prof. Andre L. Tits (University of Maryland) for providing the FORTRAN version of the FSQP algorithm gratis.

References

[1] A. Kundu, S.M. Cramer, Anal. Biochem. 248 (1997) 1–6.
[2] J. Zhu, G. Guiochon, J. Chromatogr. A 659 (1994) 15–25.
[3] P. Cysewski, A. Jaulmes, R. Lemque, B. Sebille, C. Vidal-Madjar, G. Jilge, J. Chromatogr. 548 (1991) 61–79.
[4] A. Velayudhan, Cs. Horvath, J. Chromatogr. 443 (1988) 13–29.
[5] N.K. Boardman, S.M. Partridge, Biochem. J. 59 (1955) 543–552.
[6] W. Kopaciewicz, M.A. Rounds, J. Fausnaugh, F.E. Regnier, J. Chromatogr. 266 (1983) 3–21.
[7] R.D. Whitley, R. Wachter, F. Liu, N.-H.L. Wang, J. Chromatogr. 465 (1989) 137–156.
[8] A. Velayudhan, Studies in Non-linear Chromatography, Doctoral Dissertation, Yale University, New Haven, CT, 1990.
[9] C.A. Brooks, S.M. Cramer, AIChE J. 38 (1992) 1969–1978.
[10] Y.-L. Li, N.G. Pinto, J. Chromatogr. A 658 (1994) 445–457.
[11] P. Raje, N.G. Pinto, J. Chromatogr. A 760 (1997) 89–103.
[12] S.R. Gallant, A. Kundu, S.M. Cramer, J. Chromatogr. A 702 (1995) 125–142.
[13] S.R. Gallant, S. Vunnum, S.M. Cramer, J. Chromatogr. A 725 (1996) 295–314.
[14] S.R. Gallant, A. Kundu, S.M. Cramer, Biotechnol. Bioeng. 47 (1995) 355–372.
[15] S.D. Gadam, S.R. Gallant, S.M. Cramer, AIChE J. 41 (1995) 1676–1686.
[16] H.-K. Rhee, N.R. Amundson, Chem. Eng. Sci. 29 (1974) 2049–2060.
[17] V. Natarajan, S.M. Cramer, AIChE J. 45 (1999) 27–37.
[18] J. Frenz, Ph. Van der Schriek, Cs. Horvath, J. Chromatogr. 330 (1985) 1–17.
[19] S.C.D. Jen, N.G. Pinto, J. Chromatogr. 590 (1992) 3–15.
[20] A. Felinger, G. Guiochon, J. Chromatogr. 609 (1992) 35–47.
[21] A. Kundu, K.A. Barnthouse, S.M. Cramer, Biotechnol. Bioeng. 56 (1997) 119–129.
[22] J. Zhou, A.L. Tits, User's Guide for FSQP Version 1.0B A FORTRAN Software for Solving Optimization Problems with General Inequality Constraints and Linear Equality Constraints, Generating Feasible Iterates, Technical Research Report, University of Maryland, College Park, MD.
[23] S.D. Gadam, G. Jayaraman, S.M. Cramer, J. Chromatogr. 630 (1993) 37–52.
[24] A. Kundu, Low Molecular Weight Displacers for Protein Purification in Ion Exchange Systems, Doctoral Dissertation, Rensselaer Polytechnic Institute, Troy, NY, 1990.
[25] V. Natarajan, S.M. Cramer, Sep. Sci. Tech. (2000) in press.
[26] A. Kundu, A.A. Shukla, K.A. Barnthouse, J. Moore, S.M. Cramer, BioPharm. 10 (1997) 64.